Ab initio calculations of external-field shifts of the 661-nm quadrupolar clock transition in neutral Ag atoms

Suat Topcu* and Jamil Nasser†
Laboratoire LIS Versailles, 45 Avenue des États-Unis 78035 Versailles, France

Latévi Max Lawson Daku‡
Université de Genève, Sciences II, CH-1211 Genève 4, Switzerland

Stephan Fritzsche§
Institute für Physik, Universität Kassel, Heinrich-Plett-Str. 40, D-34132 Kassel, Germany
(Received 8 February 2006; published 11 April 2006)

Frequency shifts of the Ag I $4d^{10}5s\ ^2S_{1/2}(F=0,M_F=0)$ to $4d^95s^2\ ^2D_{5/2}(F'=2,M_{F'}=0)$ electric-quadrupole transition at 330.6 nm due to external fields are calculated using multiconfigurational self-consistent field methods. As this forbidden transition is free from first order Doppler and Zeeman effects, it is under investigation for the realization of an atomic optical clock. The calculated perturbations are the light shift, the blackbody frequency shift, and the quadratic Zeeman shift. Results show that a total uncertainty of 10^{-18} could be reach without confining the atoms in a Lamb-Dicke regime in an optical lattice.

DOI: 10.1103/PhysRevA.73.042503 PACS number(s): 31.15.Ar, 06.30.Ft, 32.60.+i, 32.80.Pj

I. INTRODUCTION

An accurate measurement of time and frequency is a prerequisite not only for fundamental science, concerning for instance the changes in fundamental constants over time, measuring gravitational redshifts, and timing pulsars, but also for technologies that support broadband communication networks and navigation with global positioning systems (GPS or GALILEO). The stability and accuracy of an atomic clock is related to the quality factor Q of the reference transition on which it is based. The quest for atomic clocks with higher levels of stability and reproducibility is therefore prompting a move from the microwave to the optical region of the spectrum. In practice, forbidden optical transitions with natural linewidths around 1 Hz or less, offer potential Q factors of order 10^{15} or even higher. When compared to the Q factors ($\sim 10^{10}$) of the present caesium microwave standard as applied for the definition of the Systeme International (SI) second, such improvement could lead to a redefinition of the second in the future.

A number of different atoms are currently being investigated in various laboratories, based on forbidden transitions in cold trapped ions or neutral atoms, and over recent years there has been significant progress in both areas [1]. For the "ion" approach [2,3], for example, its a commonly shared opinion that it may lead to a better ultimate frequency accuracy while its stability will likely remain limited by the quantum projection noise. In contrast, the "atomic" approach [4] should lead to a better frequency stability thanks to the numerous quantum absorbers contributing to the signal but with an accuracy which will be limited by the Doppler shift. Recently Katori [5] proposed and demonstrated a scheme that combines the advantages of both approaches. The idea is to trap Sr neutral atoms in the Lamb-Dicke regime in a three-dimensional (3D) optical lattice operating at a "*magic*" wavelength where the light shift of the clock transition vanishes. Thanks to this subwavelength confinement, the first-order Doppler shift as well as the photon recoil shift disappear. The Sr optical lattice clock demonstrated a linewidth two orders of magnitude narrower than that observed for neutral-atom optical clocks and a stability better than that of single-ion clocks [6].

Another strategy has been chosen by groups at Garching [7] and at CNAM in Paris [8] in closed collaboration with two of us, in that the quadrupolar transition $4d^{10}5s\ ^2S_{1/2}$-$4d^95s^2\ ^2D_{5/2}$ in neutral Ag atoms is applied. The use of neutral silver atoms as a candidates for a future optical clock has been first proposed by Bender and Hall in 1976 [9]. This transition presents numerous advantages. Although accurate calculation has never been published, the $5\ ^2D_{5/2}$ metastable level has an estimated natural linewidth of about 1 Hz. This long-lived state is accessible from the ground state $5\ ^2S_{1/2}$ with a two-photon transition at 661.2 nm, providing a first-order Doppler-free interaction with atoms of all velocities [9,10]. Furthermore, the nuclear spin $I=1/2$ of the two stable isotopes ^{107,109}Ag induces a hyperfine structure which allows transitions between levels with $M_F=0$ and thus are insensitive to the first order Zeeman effect. This also permits a sub-Doppler cooling mechanism that may lead to low temperatures and narrow transverse velocity distributions. Finally, as an important technical aspect, the frequencies needed to drive the clock transition and the cooling transition ($4d^{10}5s\ ^2S_{1/2}$-$4d^{10}5p\ ^2p_{3/2}$, $\lambda=328.126$ nm) can be provided by solid state lasers based on a Nd:YLF crystal [11].

While the clock transition has no linear Zeeman shift, it does have a quadratic Zeeman shift and an ac Stark shift.

*Electronic address: suat.topcu@ens-phys.uvsq.fr
†Electronic address: jnasser@physique.uvsq.fr
‡Electronic address: Max.Lawson@chiphy.unige.ch
§Electronic address: s.fritzsche@physik.uni-kassel.de

Since none of these shifts have been measured yet, it is useful to have calculated values. In this paper, we report accurate calculations of the systematic shifts of the clock transition due to external fields as well as good estimates of the lifetime of the $5\,^2D_{5/2}$ state. The oscillator strengths, transition-matrix elements, lifetimes, and polarizabilities for several low-lying levels have been calculated. It is pointed out that this approach would allow one to reach an equivalent level of total uncertainty as the scheme proposed by Katori. All the calculations were carried out using two multiconfiguration self-consistent field (MCSCF) methods based on the Hartree-Fock (HF) and Dirac-Fock (FD) equations combined with a configuration-interaction (CI) for taking into account the core-core and core-valence correlation effects. Unless specified otherwise, we use atomic units ($|e| = \hbar = \mathrm{m}_e \equiv 1$) throughout the paper.

II. THEORY

A. Transition properties

Let **D** be the dipole-moment operator for the interaction of the atomic electrons with the radiation field. Making use of the Wigner-Eckart theorem, the line strength of an electric dipole transition between a ground state $|\gamma J\rangle$ and an excited state $|\gamma' J'\rangle$ is linked to the reduced matrix element by

$$S_{\gamma\gamma'} = |\langle \gamma J||D||\gamma' J'\rangle|^2. \tag{1}$$

Of special importance is the oscillator strength, the so-called f value, which is linked to the line strength by

$$f(\gamma J, \gamma' J') = \frac{2}{3(2J+1)} \omega_{\gamma'\gamma} S_{\gamma\gamma'} \tag{2}$$

where $\omega_{\gamma'\gamma} = E_{\gamma' J'} - E_{\gamma J}$ is expressed in hartrees and S in atomic units of $e^2 a_0^2$.

The lifetime $\tau_{\gamma' J'}$ of the level $|\gamma' J'\rangle$ is

$$\tau_{\gamma' J'} = \frac{1}{\sum_{\gamma J} A(\gamma' J', \gamma J)}, \tag{3}$$

where A is the transition rate for emission given by

$$A(\gamma' J', \gamma J) = -\frac{4}{3c^3} \frac{\omega_{\gamma'\gamma}^3}{2J'+1} S_{\gamma\gamma'}.$$

B. Computational details

In the MCHF method [12], the wave function Φ of an LS term labeled γLS, is expanded in terms of configuration state functions (CSF) with the same LS term

$$\Psi(\gamma \mathrm{LS}) = \sum_n c_n(\gamma) \Phi(\gamma_n' \mathrm{LS}), \tag{4}$$

where γ represents all further quantum numbers necessary for the unique specification of the quantum state. The CSFs are antisymmetrized products of spinorbitals

$$\phi_{nlm_l m_s}(\mathbf{r}) = \frac{1}{r} P_{nl}(r) Y_{lm_l}(\theta, \varphi) \xi_{m_s}(\sigma). \tag{5}$$

In the multiconfigurational self-consistent field (MCSF) calculations, the radial functions $P_{nl}(r)$ and the expansion coefficients $c_n(\gamma)$ are simultaneously optimized to self-consistency. Once the spinorbitals are known, relativistic effects can be taken into account by performing CI calculations within the Breit-Pauli (BP) approximation. In this framework, the atomic state functions (ASFs) are expanded over CSFs which are now eigenfunctions of the total angular momentum $\mathbf{J}^2 = (\mathbf{L}+\mathbf{S})^2$,

$$\Psi(\gamma LSJM) = \sum_n c_n(\gamma) \Phi(\gamma_n' L_n S_n JM). \tag{6}$$

The combination of the MCDF and relativistic CI methods allows a more accurate treatment of the relativistic many body problem. In this context, the function of an atomic state of parity P labeled γPJM is expanded in terms of jj-coupled CSFs of the same parity and of same J and M quantum numbers according to

$$\Psi(\gamma PJM) = \sum_n c_n(\gamma) \Phi(\gamma_n' PJM). \tag{7}$$

The CSFs are built from antisymmetrized product of relativistics spinorbitals

$$\phi_{n\kappa m}(\mathbf{r}) = \frac{1}{r} \begin{pmatrix} P_{n\kappa}(r) \chi_{\kappa m}(\hat{\mathbf{r}}) \\ \mathrm{i} Q_{n\kappa}(r) \chi_{-\kappa m}(\hat{\mathbf{r}}) \end{pmatrix}. \tag{8}$$

The quantity κ is the relativistic angular quantum number: $\kappa = \pm(j+1/2)$ for $l = j \pm 1/2$. $P_{n\kappa}(r)$ and $Q_{n\kappa}(r)$ are called the small and large component of the radial wave functions with $\chi_{\kappa m}(\hat{\mathbf{r}})$ being a spinor spherical harmonic in the lsj coupling scheme

$$\chi_{\kappa m}(\hat{\mathbf{r}}) = \sum_{m_l, m_s} \left\langle l \frac{1}{2} m_l m_s | jm \right\rangle Y_{lm_l}(\theta, \varphi) \xi_{m_s}(\sigma). \tag{9}$$

In the MCDF approach, the Dirac-Coulomb Hamiltonian

$$H_{\mathrm{DC}} = \sum_i \left[c \alpha_i \cdot \mathbf{p}_i + (\beta_i - 1) c^2 - \frac{Z}{r_i} \right] + \sum_{i>j} \frac{1}{r_{ij}} \tag{10}$$

is used to perform the MCSCF calculations. The optimized spinorbitals can be used then to carry out relativistic CI calculations using a Hamiltonian that can include other interaction operators which have been omitted in Eq. (10). The most important is the transverse photon interaction operator

$$H_{\mathrm{trans}} = -\sum_{i<j} \left[\frac{\alpha_i \cdot \alpha_j \cos(\omega_{ij} r_{ij})}{r_{ij}} + (\alpha_i \cdot \nabla_i) \times (\alpha_j \cdot \nabla_j) \frac{\cos(\omega_{ij} r_{ij}) - 1}{\omega_{ij}^2 r_{ij}} \right] \tag{11}$$

which, in the low-frequency limit $\omega_{ij} \to 0$, is referred to as the Breit operator. The lowest-order nuclear motional corrections, the dominant quantum-electrodynamical corrections, that is, the self-energy and the vacuum polarization, may be included as well.

Below, we used the ATSP program [13] for the MCHF and the BP+CI calculations, while the GRASP92 program [14] was applied for the MCDF computations. The subsequent CI calculations were performed by means of the RELCI component of the RATIP package [15]. In these computations, the Breit interaction along with the vacuum polarization were included in the CI calculations. We also used a semiempirical relativistic Hartree-Fock (RHF) approach described by Cowan [16]. Although, this method suffers from the drawback that the core-core and core-valence correlations are not taken into account, it has the great advantage of being simple to use and that it does not require high-performance computers.

It is difficult to say which method has the best accuracy without having reliable experimental data available. However, it is commonly shared that the MCSCF methods give better results than the RHF one. Furthermore, in this paper, very large scale multiconfigurational calculations have been performed only with the MCDF+CI. Hence, we expect that the values obtained by this method are the most reliable ones. The results of the two other methods are reported only for purpose of comparison.

III. ENERGIES, LIFETIMES, AND SPECTROSCOPIC PROPERTIES OF THE LOW-LYING LEVELS

For the RHF approach, the configuration interaction integrals for all electron configurations were fixed at 0.85 of their HF values. The exchange integrals, spin-orbit integrals as well as the averaged energy of the relevant configurations were let to vary in the process of fitting the state energies. For energy fitting, we use experimental values of the excited state energies from Ref. [17]. The MCHF calculations were carried out for the ground $4d^{10}5s\ ^2S$ LS term and for the excited terms $4d^{10}5p\ ^2P$ and $4d^9 5s^2\ ^2$D. They led to the orbital set consisting of the $\{1s,2s,2p,3s,3p,3d,4s,4p,4d,4f,5s,5d\}$ orbitals which was then used to perform the BP+CI calculations for characterizing the $5\ ^2S_{1/2}$ ground state and the four lowest-lying excited states $n=5\ ^2P_{1/2}$, $^2P_{3/2}$, $^2D_{3/2}$, and $^2D_{5/2}$. For both the MCHF and the BP+CI calculations, tens of CSFs were appropriately generated by single (S) and double (D) excitations from the reference configuration $4d^{10}5s$, $4d^{10}5p$, and $4d^9 5s^2$. The MCDF calculations allowed to obtain a final orbital set which consists of the orbitals $\{1s_{1/2}$, $2s_{1/2}$, $2p_{1/2}$, $2p_{3/2}$, $3s_{1/2}$, $3p_{1/2}$, $3p_{3/2}$, $3d_{3/2}$, $3d_{5/2}$, $4s_{1/2}$, $4p_{1/2}$, $4p_{3/2}$, $4d_{3/2}$ $4d_{5/2}$, $4f_{5/2}$, $4f_{7/2}$, $5s_{1/2}$, $5p_{1/2}$, $5p_{3/2}$, $5d_{3/2}$, $5d_{5/2}$, $6p_{1/2}$, $6p_{3/2}$, $6d_{3/2}$, $6d_{5/2}$, $7s_{1/2}$, $7p_{1/2}$, and $7p_{3/2}\}$ orbitals. Using the extended optimal level EOL option of the GRASP92 code, these orbitals were optimized by minimizing the energy functional given by the average of the energies of the $^2S^e_{1/2}$ ground state and the four lowest-lying excited states $^2P^o_{1/2}$, $^2P^o_{3/2}$, $^2D^e_{3/2}$, and $^2D^e_{5/2}$. The calculations were performed in several steps wherein the CSFs were generated by SD excitations from the relativistic reference configurations $4d^4_{3/2}4d^6_{5/2}5s_{1/2}$, $4d^4_{3/2}4d^6_{5/2}5p_{1/2}$, $4d^3_{3/2}4d^6_{5/2}5s^2$, and $4d^4_{3/2}4d^5_{5/2}5s^2\ J=1/2$, $3/2$, $5/2$. We considered first all orbitals up to the $n=4$ shell excepted the $4f_{5/2}$ and $4f_{7/2}$ ones. Thereafter, we systematically increased the size of the orbital set while keeping the $n=\{1-3\}$ and $4s_{1/2}$, $4p_{1/2}$, and $4p_{3/2}$ orbitals fixed.

For most of the CI calculations following the MCDF ones, the CSFs were generated from the same reference configurations as for the MCDF calculations, by allowing SD and also triple (T) excitations of the valence electrons into the $n=5$, $n=6$, and $n=7$ shells. These excitation schemes will be referred to by the nSD and nSDT notations, and the sets of CSFs which they lead to by $\{n\text{SD}\}$ and $\{n\text{SDT}\}$. In these calculations, the core is defined by the filled $n=\{1-3\}$ and $4s_{1/2}$, $4p_{1/2}$, and $4p_{3/2}$ subshells. In the other CI calculations that have been carried out, the core was defined by the filled $n=\{1-3\}$ shells in order to allow the polarization of the $4s_{1/2}$, $4p_{1/2}$, and $4p_{3/2}$ "semicore" electrons by the valence electrons. In this case, the CSFs were obtained from the same reference configurations by considering only SD excitations into the $n=7$ shell; this excitation scheme will be referred to as $7\text{SD}'$. We estimated an accuracy of few percent for the electric dipole matrix elements. The difference in the calculated properties due to the mass shift between the two isotopes ^{107}Ag and ^{109}Ag are less than the uncertainties. The data used for the numerical evaluations are from the ^{109}Ag isotope.

Table I gives the energies of the ground state $^2S^e_{1/2}$ and the calculated values of the energy ΔE of the lowest-lying excited states $n=5\ ^2p^o_{1/2}$, $^2P^o_{3/2}$, $^2D^e_{3/2}$, and $^2D^e_{5/2}$ with regard to the energy of the ground state and as functions of the number n_c of CSFs involved in the MCDF+CI calculations. When only valence correlations were considered, convergence of the energy of the five states is achieved by combining the {6SDT} and {7SD} CSF sets. No further improvement is achieved if triple excitations into the $n=7$ shell are included as seen from the results obtained for the {7SDT} set. In fact, the incorporation of triple excitations by passing from the {5SD} to the {5SDT} set or from a $\{n\text{SDT}\}\cup\{(n+1)\text{SD}\}$ to a $\{(n+1)\text{SDT}\}$ set $(n=5,6)$, tend to have less influence on the energies than the inclusion of SD excitations into the upper shell by passing from a $\{n\text{SDT}\}$ to a $\{n\text{SDT}\}\cup\{(n+1)\text{SD}\}$ set. From the CI calculations performed with $\{7\text{SD}'\}$ set, we found a quite large decrease of the energies of the states which shows that the polarization of the electrons from the $4s_{1/2}$, $4p_{1/2}$, and $4p_{3/2}$ semicore subshells by the valence electrons must be taken into account. Further improvements are achieved when one adds to this set, triple excitations from the valence electrons into the $n=6$ shell. Experimental results are also shown for purpose of comparison. One notes that the results obtained are in satisfactory agreement with experiment since the MCDF ΔE values differ from the experimental values by only $-2379\ \text{cm}^{-1}$ (-8.1%) and $-2364\ \text{cm}^{-1}$ (-7.8%), respectively, for the $^2P^o_{1/2}$ and $^2P^o_{3/2}$ levels, and by only $+2022\ \text{cm}^{-1}$ (6.7%) and $+2133\ \text{cm}^{-1}$ (6.1%) for the $^2D^e_{5/2}$ and $^2D^e_{3/2}$, respectively. For the CI calculations that includes Breit interaction and vacuum polarization, the results tend to be worse than the MCDF ones if one only deals with valence correlation. The semicore-valence correlation (using the $\{6\text{SDT}\}\cup\{7\text{SD}'\}$ basis set) must be considered in order to obtain results which are in very good agreement with experiment. In this case, the calculated ΔE values differ from the experimental values by only $-2030\ \text{cm}^{-1}$ (-6.9%) and $-2062\ \text{cm}^{-1}$ (-6.8%) respectively for the $^2P^o_{1/2}$ and $^2P^o_{3/2}$

TABLE I. Calculated values of the energy E (Hartree) of the ground state and the lowest-lying excited states as functions of the number n_c of CSFs involved in the CI calculations. Calculated values of the energy ΔE (cm^{-1}) of the states with respect to the energy of the ground state as functions of the number n_c of CSFs involved in the MCDF and CI calculations. Experimental values from Ref. [17] are also reported.

	$^2S^e_{1/2}$		$^2P^o_{1/2}$		$^2P^o_{3/2}$		$^2D^e_{5/2}$		$^2D^e_{3/2}$	
Basis set	n_c	E	n_c	ΔE	n_c	ΔE	n_c	ΔE	n_c	ΔE
MCDF calculation										
{7SD}	2161	0	2532	27173	4387	28109	4399	32265	3732	36847
CI calculation, valence correlation										
{5SD}	521	−5311.659	555	23684	981	24695	1132	81759	923	86078
{5SDT}	7237	−5311.663	9090	23824	16558	24768	16789	36924	13142	41217
{5SDT}∪{6SD}	7707	−5311.694	9600	27169	17439	28073	17728	33632	13948	37945
{6SDT}	16932	−5311.696	22239	27307	40090	28167	38128	33492	30406	37789
{6SDT}∪{7SD}	17568	−5311.701	22954	27445	41313	28275	39372	33057	31491	37370
{7SDT}	33048	−5311.701	44663	27483	79881	28308	72816	33005	58869	37315
CI calculations, including valence and semicore-valence correlation										
{7SD′}	8370	−5311.842	7064	27186	11866	28159	16053	29427	14137	33911
{6SDT}∪{7SD′}	24309	−5311.847	28238	27522	50094	28411	52110	29844	42814	34293
Experiment				29552		30473		30243		34714

levels, and by only $-399\ cm^{-1}$ (-1.3%) and $-421\ cm^{-1}$ (-1.2%) for the $^2D^e_{5/2}$ and $^2D^e_{3/2}$, respectively.

Table II gives the calculated values of the reduced matrix elements between the ground state and the $4d^{10}\ np\ ^2P_{1/2;3/2}$ states and between the upper state and the $4d^{10}\ np\ ^2P_{3/2}$ states. Table III summarizes the values of the Einstein coefficient, lifetime, and width of the clock transition obtained by the different methods.

IV. LIGHT SHIFT, BLACKBODY RADIATION, AND OTHER SYSTEMATIC ERRORS AFFECTING THE CLOCK TRANSITION

A. Light shift of atomic hyperfine levels

Within a laser field $\vec{\xi}(\omega_L,\vec{\epsilon})$, the transition frequency between the states $|\gamma JFM_F\rangle$ and $|\gamma J'F'M_{F'}\rangle$ is subjected to an ac Stark shift given by

$$\omega_{obs}=\omega_0-\Delta\alpha(\omega_L,\vec{\epsilon})|\vec{\xi}(\omega_L,\vec{\epsilon})|^2/4\hbar+O(\vec{\xi}^4), \tag{12}$$

where ω_0 the unperturbed atomic resonance frequency and $\Delta\alpha(\omega_L,\vec{\epsilon})$ denotes the differential ac dipole polarizability. In the case where the laser field is linearly polarized along the z axis, the Stark Hamiltonian H_{EE} is, in the second-order perturbation theory, given by [18,19]

$$\begin{aligned}H_{EE}=&-\frac{1}{4}\alpha^{(0)}|\gamma J\rangle|\ \xi_z)|^2-\frac{1}{4}\alpha^{(2)}|\gamma J\rangle\\&\times\sum_{FM_FF'M_{F'}}|FM_F\rangle\langle F'M_{F'}|\times|\xi_z|^2\begin{pmatrix}1&2&1\\0&0&0\end{pmatrix}\\&\times\left[\frac{15(J+1)(2J+1)(2J+3)}{2J(2J-1)}\right]^{1/2}\\&\times(-1)^{I+J+F-F'-M_F}\sqrt{(2F+1)(2F'+1)}\\&\times\begin{pmatrix}F&2&F'\\M_F&0&-M_{F'}\end{pmatrix}\begin{Bmatrix}F&2&F'\\J&I&J\end{Bmatrix}.\end{aligned} \tag{13}$$

The scalar polarizability $\alpha^{(0)}$ shifts all hyperfine and magnetic sublevels equally. The tensor polarizability $\alpha^{(2)}$ mixes the hyperfine and magnetic sublevels. The dynamic $E1$ scalar polarizability and tensor polarizability of the level $|\gamma J\rangle$ are given by

$$\alpha^{(0)}|\gamma J\rangle=\frac{2/\hbar}{3(2J+1)}\sum_{\gamma'J'}|\langle\gamma J||D||\gamma'J'\rangle|^2\frac{\omega_{\gamma\gamma'}}{\omega^2_{\gamma\gamma'}-\omega^2_L} \tag{14}$$

and

$$\begin{aligned}\alpha^{(2)}|\gamma J\rangle=&\frac{4}{\hbar}\left[\frac{5J(2J-1)}{6(J+1)(2J+1)(2J+3)}\right]^{1/2}\\&\times\sum_{\gamma'J'}(-1)^{J+J'}\begin{Bmatrix}J&1&J'\\1&J&2\end{Bmatrix}|\langle\gamma J||D_q||\gamma'J'\rangle|^2\\&\times\frac{\omega_{\gamma\gamma'}}{\omega^2_{\gamma\gamma'}-\omega^2_L}.\end{aligned} \tag{15}$$

In these formulas, ω_L is assumed to be at least several linewidths off resonance with the corresponding transition. This condition is satisfied for the frequencies considered in this work. We calculate the light shifts of the transitions from the $4d^{10}5s\ ^2S_{1/2}(F=0\ M_F=0)$ sublevel to the $4d^95s^2\ ^2D_{5/2}(F'=2\ M_{F'}=0)$ sublevel. The Stark energy of the $5\ ^2D_{5/2}$ state is produced by the scalar and tensor polarizabilities whereas only scalar polarizability contribute to the Stark energy of the ground state (this is due to $J<1$). The calculations of the

TABLE II. Reduced matrix elements between the low-lying states of neutral silver atoms (in a.u.).

	$(S_{\gamma\gamma'})^{1/2}$		
n	RHF	MCDF	MCHF
	$4d^{10}5s\ ^2S_{1/2}$-$4d^{10}np\ ^2P_{1/2}$		
5	2.71626	3.15676	3.10948
6	0.25713	0.28695	0.55130
7	0.07804	0.46984	0.27075
8	0.02411		
9	0.00753		
10	0.00824		
	$4d^{10}5s\ ^2S_{1/2}$-$4d^{10}np\ ^2P_{3/2}$		
5	3.84198	4.39435	4.39814
6	0.35436	0.76091	0.77914
7	0.10750	0.20103	0.38288
8	0.03408		
9	0.00753		
10	0.06839		
	$4d^{10}np\ ^2P_{3/2}$-$4d^{10}5s^2\ ^2D_{5/2}$		
5	0.53457	0.46459	0.52186
6	0.25828	0.29357	0.52555
7	0.19293	0.21712	0.175630
8	0.14554		
9	0.10885		
10	0.11751		

ac polarizabilities of the $5\ ^2S_{1/2}$ and $5\ ^2D_{5/2}$ incorporate, respectively, the coupling with the states states $np\ ^2P_{1/2,3/2}$ and $np\ ^2P_{3/2}$. We perform a RHF calculation of the reduced matrix elements for the states $np\ ^2P_{1/2,3/2}$ for $n=\{5-10\}$. Results show that the $|\langle 5\ ^2S_{1/2}||D||5\ ^2P_{1/2,3/2}\rangle|$ contribute for 95% of the ground state polarizability and the $|\langle 5\ ^2D_{5/2}||D||5\ ^2P_{3/2}\rangle|$ element contribute for 61% of the upper state polarizability. Figure 1 represents the scalar polarizabilities of both levels as functions of laser wavelength.

More accurate calculations have been performed for $n\leqslant 7$ using the MLTPOL program [20] with the wave functions issue from MCHF+BP+CI calculation and by means of RELCI program [21] with the wave functions issue from MCDF+CI calculation. Using the MCDF+CI value for $\lambda_L=661.2$ nm, we obtain for the scalar polarizabilities $\alpha^{(0)}|^2S_{1/2}\rangle=42.474\,85\times10^{-4}$ (Hz m^2)/W, $\alpha^{(0)}|^2D_{5/2}\rangle=23.586\,21\times10^{-6}$ (Hz m^2)/W, and for the tensor polarizability $\alpha^{(2)}|^2D_{5/2}\rangle=-\alpha^{(0)}|^2D_{5/2}\rangle$. When compared to the $E1$ scalar polarizability α^{E1}, the higher orders multipole corrections from the magnetic dipole $M1$ and the electric-quadrupole $E2$ were found negligible. Numerical estimates give $\alpha^{E2}\approx\alpha^{M1}\approx10^{-10}\alpha^{E1}$ for both levels. The resulting frequency shift is then given by

$$\delta\omega_0/2\pi\ (\mathrm{Hz}) = -1.421\,21\times10^{-3}(P/S)\ (\mathrm{W/m^2}). \quad (16)$$

The values obtained by the MCHF+BP+CI and RHF method are, respectively, $-1.416\,16\times10^{-3}$ (Hz m^2)/W and $-1.063\,14\times10^{-3}$ (Hz m^2)/W. One can notice a good agreement between the value obtained by the MCDF and MCHF methods. The value obtained by the RHF method is lower but still in good agreement with the other results. This could easily be explained if we take into account that the core-core and core-valence effects are not considered in this method. This frequency shift can be reduced below to 10^{-18} in relative value if the laser intensity fluctuations are below to 1 W/cm^2. Figure 2 gives the light shift of the transition from the $5\ ^2S_{1/2}(F=0,M=0)$ sublevel to the $5\ ^2D_{5/2}(F'=2,M_{F'}=0)$ sublevel as a function of the laser field intensity. The value of the wavelength of the laser field is chosen to be $\lambda=661.2$ nm.

TABLE III. Transition probabilities, lifetime, and width of the quadrupolar clock transition of the silver atom.

Method	A (s^{-1})	Lifetime (s)	Width (Hz)
RHF	5.026	0.199	0.799
MCHF+BP+CI	5.747	0.174	0.915
MCDF+CI	8.680	0.115	1.381

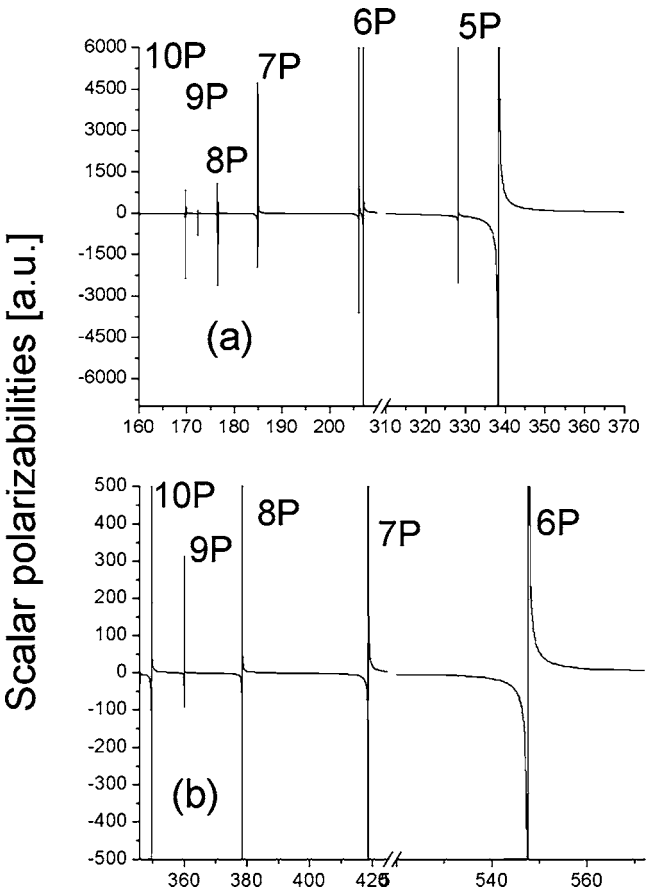

FIG. 1. Scalar polarizabilities $\alpha^{(0)}$ of the ground state $5S_{1/2}$ (a) and the excited state $5D_{5/2}$ (b) as a function of the light wavelength λ_L.

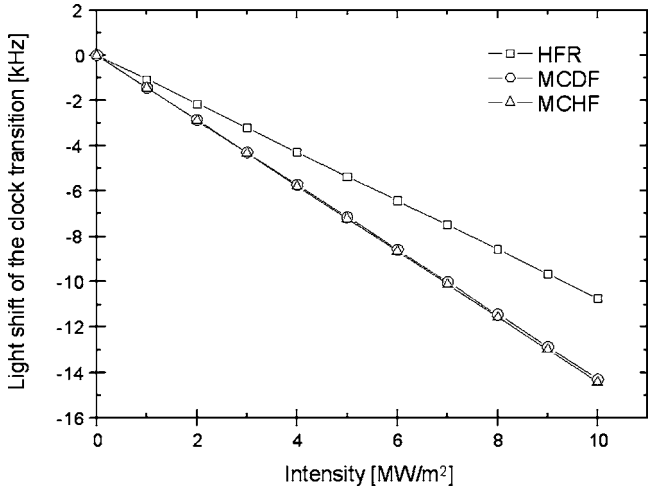

FIG. 2. Light shift of the transition from the $5S_{1/2}F=0$, $M_F=0$ sublevel to the $5D_{5/2}F'=2$, $M_{F'}=0$ sublevel. The value of the wavelength of the laser field is chosen to be $\lambda=661.2$ nm. The electric component field is linearly polarized along the quantization axis z.

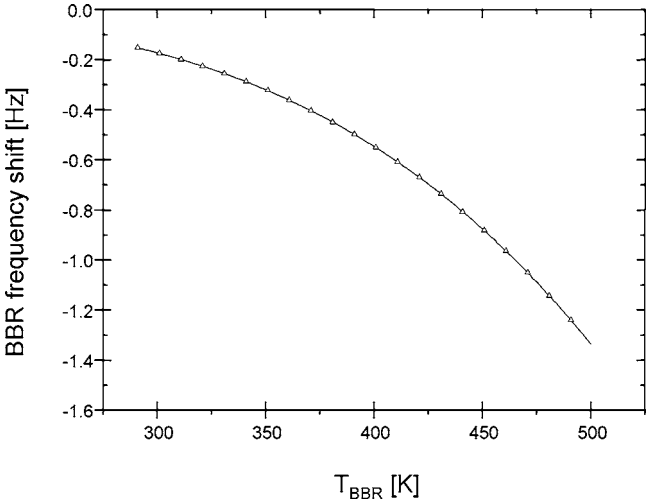

FIG. 3. Predicted frequency shifts due to BBR as a function of temperature T_{BBR}.

B. Blackbody radiation

The interaction between atoms and the electric fields of blackbody radiation (BBR) both induces transitions and produces non resonant Stark and Zeeman shifts of the atomic transitions [22]. The nonresonant ac Stark shift $\Delta W^{(k)}$ of the energy of state $|\gamma J\rangle$ induced by the level $|\gamma' J'\rangle$ is given by [23]

$$\Delta W^{(k)}|\gamma J\rangle = -\frac{1}{\hbar}\sum_{\gamma'} S_{\gamma\gamma'}\int_0^{+\infty}\frac{\omega_{\gamma\gamma'}}{\omega_{\gamma\gamma'}^2-\omega^2}\xi^2(\omega)d\omega, \quad (17)$$

where e is the electron charge and $\xi^2(\omega)$ is the quadratic electric field strength of BBR. At room temperature ($T=300$ K), BBR has its peak spectral density around a frequency $\omega_{\max}/2\pi=17$ THz which is far below the minimum value of $\omega_{\gamma\gamma'}$ corresponding to the $D1$ and $D2$ transitions in silver atoms. Hence, it is possible to omit the ω^2 term in the denominator of Eq. (17) avoiding the singularity of the integrand [24]. It is assumed that the perturbing BBR is isotropic and unpolarized. Only the scalar polarizability contributes to the BBR shift. Furthermore, due to the very low intensity of the BBR field, the hyperpolarizability effect is negligible. The relation (17) becomes

$$\Delta W^{(k)}|\gamma J\rangle = -\frac{1}{2}\alpha_0|\gamma J\rangle\langle\xi_\omega^2(t)\rangle, \quad (18)$$

where

$$\alpha_0|\gamma J\rangle = \frac{2}{\hbar}\sum_{\gamma'}\frac{S_{\gamma\gamma'}}{\omega_{\gamma\gamma'}} \quad (19)$$

is the dc Stark coefficient. The time averaged quadratic electric field strength is given by the Stephan-Boltzman law

$$\langle\xi_\omega^2(t)\rangle = \int_0^{+\infty}\xi^2(\omega)d\omega = \frac{4\sigma T^4}{\varepsilon_0 c}. \quad (20)$$

The total BBR shift between two states $|\gamma J\rangle$ and $|\gamma' J'\rangle$ is then

$$\Delta\omega = -\frac{1}{\hbar}(\Delta W|\gamma' J'\rangle - \Delta W|\gamma J\rangle). \quad (21)$$

As previously, the summation occurs, respectively, on the $np\,^2P_{1/2,3/2}$ and $np\,^2P_{3/2}$ $n=\{5-7\}$ for the ground state and the upper state, with the wave functions issue from the MCDF+CI calculations. We obtained $\alpha_0|^2S_{1/2}\rangle=7.16\times10^{-39}$ (C m^2)/V and $\alpha_0|^2D_{5/2}\rangle=6.83\times10^{-39}$ (C m^2)/V. Combining both results, the total BBR frequency shift expressed as a relative quantity is given by

$$y_{BBR} = \Delta\omega(T)/\omega_0 = \beta\chi(T/300\text{ K})^4 \quad (22)$$

with $\beta=1.9\times10^{-16}$ and $\chi=1+0.001\,(T/300\text{ K})^2$. Here ω_0 is the unperturbed clock transition frequency of the silver atoms, χ is a corrective term which accounts for the separation in frequency between the BBR spectrum and the transition frequency of the $D1$ and $D2$ lines in silver atoms [24]. The blackbody frequency shift in the clock transition is estimated to be -160 mHz at $T=293$ K. The quantity y_{BBR} can be reduced to the 10^{-18} level by controlling the surrounding temperature variation $\Delta T\leqslant0.5$ K. Figure 3 gives the variation of the frequency shift of the clock transition as a function of the temperature T_{BBR}.

C. Quadratic Zeeman shift

While the $(F=0,M_F=0)$ to $(F'=2,M_{F'}=0)$ hyperfine component has no linear Zeeman shift, it does have a quadratic Zeeman shift that must be accounted for. Let H_S and H_D be the effective Hamiltonian operators that operate within the subspaces of hyperfine sublevels associated with the levels $5\,^2S_{1/2}$ and $5\,^2D_{5/2}$, respectively,

$$H_S = hA_S \mathbf{I}\cdot\mathbf{J} + g_J(S)\mu_B \mathbf{J}\cdot\mathbf{B} + g_I'\mu_B \mathbf{I}\cdot\mathbf{B},$$

$$H_D = hA_D \mathbf{I}\cdot\mathbf{J} + g_J(D)\mu_B \mathbf{J}\cdot\mathbf{B} + g_I'\mu_B \mathbf{I}\cdot\mathbf{B}, \qquad (23)$$

where A_S and A_D are the dipole hyperfine constants and μ_B is the Bohr magneton. All of the parameters entering in H_S and H_D are known from experiments. The ground-state hyperfine constant A and the excited-state hyperfine constant A_D have been measured in Ref. [25,26] to be, respectively, 1976.93(4) and −145.1584(5) MHz. For low magnetic fields (B less than 1 mT), it is sufficient to calculate the energy levels to second order in B. To this order in B, the energies of the hyperfine-Zeeman sublevels for the states denoted $|\gamma \mathrm{JFM}_F\rangle$ are

$$\langle 5s\ 1/2\ 0\ 0|H_S|5s\ 1/2\ 0\ 0\rangle = E_S - \frac{3hA_S}{4} - \frac{(g_J - g_I')^2\mu_B^2 B^2}{4hA_S},$$

$$\langle 5s^2\ 5/2\ 2\ 0|H_D|5s^2\ 5/2\ 2\ 0\rangle = E_D - \frac{7hA_D}{4} - \frac{(g_J - g_I')^2\mu_B^2 B^2}{12hA_D}, \qquad (24)$$

where E_S and E_D are the unperturbed energy levels of the corresponding states. We obtained −993.32(2) $\mathrm{Hz/G^2}$ for the ground state and 1621.02(1) $\mathrm{Hz/G^2}$ for the upper state. This leads to a total shift of 627.70(2) $\mathrm{Hz/G^2}$. To reach a relative accuracy of 10^{-18}, one has to control the surrounding magnetic field within 1 mG which is currently the case in Cs atomic clocks.

V. SUMMARY AND CONCLUSION

We report *ab initio* calculations of the frequency shifts of the quadrupolar optical clocks transition in neutral silver atoms due to external fields. We found that the fractional frequency shift due to the laser field can be reduced to 10^{-18} if the laser intensity fluctuations are within 0.1 $\mathrm{mW/cm^2}$. The BBR frequency shift is equal to −160 mHz at $T=293$ K. Fractional BBR shift can be reduced to 10^{-18} by controlling the fluctuations of the surrounding medium temperature to $\Delta T \leqslant 0.5$ K. The effect of the quadrupolar Zeeman shift can also be negligible ($\leqslant 10^{-18}$) if the magnetic field variations of the surrounding medium are within $\Delta B \leqslant 1$ mG. The lifetime of the upper metastable level has been evaluated to $\tau = 115$ ms. Hence, the neutral silver atom appears as a promising candidate for the next generation of atomic optical clocks. Recently, this transition has been observed for the first time by the group at CNAM using a thermal atomic beam [27].

ACKNOWLEDGMENT

We are grateful to Stephane Guerandel for the helpful discussions concerning the Cowan's code.

[1] S. A. Diddams, J. C. Bergquist, S. R. Jefferts, and C. W. Oates, Science **306**, 1318 (2004).
[2] H. S. Margolis, G. P. Barwood, G. Huang, H. A. Klein, S. N. Lea, K. Szymaniec, and P. Gill, Science **306**, 1355 (2004).
[3] W. H. Oskay, W. M. Itano, and J. C. Bergquist, Phys. Rev. Lett. **94**, 163001 (2005).
[4] C. W. Hoyt, Z. W. Barber, C. W. Oates, T. M. Fortier, S. A. Diddams, and L. Hollberg, Phys. Rev. Lett. **95**, 083003 (2005).
[5] M. Takamoto, F. L. Hong, R. Higashi, and H. Katori, Nature (London) **435**, 321 (2005).
[6] A. D. Ludlow, M. M. Boyd, T. Zelevinsky, S. M. Foreman, S. Blatt, N. Notcutt, T. Ido, and J. Ye, Phys. Rev. Lett. **96**, 033003 (2006).
[7] G. Uhlenberg, J. Dirscherl, and H. Walther, Phys. Rev. A **62**, 063404 (2000).
[8] T. Badr, S. Guerandel, M. D. Plimmera, P. Juncar, and M. E. Himbert, Eur. Phys. J. D **14**, 39 (2001).
[9] P. L. Bender, J. L. Hall, R. H. Garstang, F. M. J. Pichanick, W. W. Smith, R. L. Barger, and J. B. West, Bull. Am. Phys. Soc. **21**, 599 (1976).
[10] W. M. Itano, J. C. Bergquist, R. G. Hulet, and D. J. Wineland, Phys. Rev. Lett. **59**, 2732 (1987).
[11] Y. Louyer, P. Juncar, M. D. Plimmer, T. Badr, F. Balembois, P. Georges, and M. E. Himbert, Appl. Opt. **43**, 1773 (2004).
[12] C. Froese Fischer, T. Brage, and P. Johnsson, *Computational Atomic Structure: An MCHF Approach* (Taylor & Francis, London, 1997).
[13] C. Froese Fischer, Comput. Phys. Commun. **128**, 635 (2000).
[14] F. A. Parpia, C. Froese Fischer, and I. P. Grant, Comput. Phys. Commun. **94**, 249 (1996).
[15] S. Fritzsche, J. Electron Spectrosc. Relat. Phenom. **114–16**, 1155 (2001).
[16] R. D. Cowan, *The Theory of Atomic Structure and Spectra* (University of California Press, Berkeley, 1981).
[17] J. C. Pickering and V. Zilio, Eur. Phys. J. D **13**, 181 (2001).
[18] F. L. Kien, V. I. Balykin, and K. Hakuta, J. Phys. Soc. Jpn. **74**, 910 (2005).
[19] The vector light shift vanishes if the laser beams are not circular polarized. Using a polarizer with an extinction ratio of 10^{-5} could guarantee a residual vector light shift less than 1 mHz on the clock transition (see Ref. [5]).
[20] C. Froese Fischer, Comput. Phys. Commun. **64**, 369 (1991).
[21] S. Fritzsche, C. Froese Fischer, and G. Gaigalas, Comput. Phys. Commun. **148**, 103 (2002).
[22] T. F. Gallagher and W. E. Cooke, Phys. Rev. Lett. **42**, 835 (1979).
[23] C. H. Townes and A. L. Schawlow, *Microwave Spectroscopy* (Dover, New York, 1975).
[24] W. M. Itano, L. L. Lewis, and D. J. Wineland, Phys. Rev. A **25**, R1233 (1982).
[25] A. G. Blachlan, D. A. Landman, and A. Lurio, Phys. Rev. **150**, 59 (1966).
[26] G. Wessel and H. Lew, Phys. Rev. **92**, 641 (1953).
[27] T. Badr (private communication), electronic address: thomas.badr@cnam.fr.